Increasing Collagen to Bioink Drives Mesenchymal Stromal Cells-Chondrogenesis from Hyaline to Calcified Layers

Océane Messaoudi, Christel Henrionnet, Edwin-Joffrey Courtial, Laurent Grossin, Didier Mainard, Laurent Galois, Damien Loeuille, Christophe Marquette, Pierre Gillet, Astrid Pinzano

Increasing collagen to bioink drives MSCs-chondrogenesis from hyaline to calcified layers.

Océane MESSAOUDI[1], PhD, oceane.mess.96@gmail.com (ORCID)0000-0002-0551-4014
Christel HENRIONNET[1], PhD, christel.henrionnet@univ-lorraine.fr (ORCID)0000-0001-7484-0377
Edwin-Joffrey COURTIAL[2], PhD, edwin.courtial@univ-lyon1.fr (ORCID) 0000-0001-7484-0377
Laurent GROSSIN[1], PhD, laurent.grossin@univ-lorraine.fr (ORCID)0000-0001-6761-0936
Didier MAINARD[1,3], PhD, MD, didier.mainard@univ-lorraine.fr (ORCID)0000-0003-1944-1538
Laurent GALOIS[1,3], PhD, MD, l.galois@chru-nancy.fr (ORCID)0000-0002-0457-4189
Damien LOEUILLE[1,4], PhD, MD, d.loeuille@chru-nancy.fr (ORCID)0000-0001-8204-5701
Christophe MARQUETTE[2], PhD, christophe.marquette@univ-lyon1.fr (ORCID)0000-0003-3019-0696
Pierre GILLET[1,5]*, PhD, MD, pierre.gillet@univ-lorraine.fr (ORCID)0000-0003-3019-0696
Astrid PINZANO[1], PhD astrid.pinzano@univ-lorraine.fr (ORCID)0000-0002-3867-2676

1. Université de Lorraine, CNRS, IMoPA, F54000 Nancy, France

2. Plateforme 3D Fab, UMR 5246 CNRS Université de Lyon, INSA, CPE-Lyon, ICBMS, 69100 Villeurbanne, France

3. Department of Orthopedic Surgery, University Hospital of Nancy, 54000, Nancy, France.

4. Department of Rheumatology, University Hospital of Nancy, 54500, Vandœuvre-Lès-Nancy, France

5. Department of Pharmacology, Toxicology & Pharmacovigilance, University Hospital of Nancy, 54500 Vandœuvre-Lès-Nancy, France.

* Corresponding author: pierre.gillet@univ-lorraine.fr

Running title

Type I collagen-enriched bioink for cartilage bioprinting

Keywords

Cartilage engineering, 3D bioprinting, human mesenchymal stromal cells, bio-ink, collagen.

Abstract (200 words)

The bioextrusion of mesenchymal stromal cells (MSCs) directly seeded in a bioink enables the production of 3D constructs, promoting their chondrogenic differentiation. Our study aimed to evaluate the effect of different type I collagen concentrations in the bioink on MSCs' chondrogenic differentiation. We printed 3D constructs using an alginate, gelatin, and fibrinogen-based bioink cellularized with MSCs, with four different quantities of type I collagen addition (0.0, 0.5, 1.0, and 5.0 mg per bioink syringe). We assessed the influence of the bioprinting process, the bioink composition, and the growth factor (TGF-β1) on the MSCs' survival rate. We confirmed the biocompatibility of the process and the bioinks' cytocompatibility. We evaluated the chondrogenic effects of TGF-β1 and collagen addition on the MSCs' chondrogenic properties through macroscopic observation, shrinking ratio, RT-PCR, glycosaminoglycan synthesis, histology, and type II collagen immunohistochemistry. The bioink containing 0.5 mg of collagen produces the richest hyaline-like extracellular matrix, presenting itself as a promising tool to recreate the superficial layer of hyaline cartilage. The bioink containing 5.0 mg of collagen enhances the synthesis of a calcified matrix, making it a good candidate for mimicking the calcified cartilaginous layer. Type I collagen thus allows the dose-dependent design of specific hyaline-cartilage layers.

Impact Statement

- 3D bioextrusion is a promising cartilage tissue engineering tool.
- We investigated different bioink type I collagen concentrations on MSC chondrogenicity.
- We used four different bioinks to print hydrogels.
- We confirmed bioink biocompatibility and cytocompatibility for MSC chondrogenicity.
- Type I collagen enables the dose-dependent design of specific hyaline-cartilage layers.

1. Introduction

Four zones of articular cartilage are distinguished by cell morphology, extracellular matrix (ECM), and collagen fiber orientation. Articular cartilage lacks nerves and blood vessels, limiting its ability to self-repair. If left untreated, hyaline joint focal lesions caused by trauma or overload degenerate into osteoarthritis (OA)[1]. This disease is becoming more prevalent because of aging, obesity, and genetic predispositions[2]. OA causes inflammation and destruction of the articular cartilage: current medical care focuses on symptom and pain relief[3,4], with treatments such as abrasion, microfracture, autologous chondrocyte implantation (ACI), and mosaicplasty used to treat focal lesions[5]. Fibrous repair tissue is only a temporary solution[6,7]. Cartilage tissue engineering (TE) provides an alternative by combining a cell contingent, a scaffold, and environmental factors to produce a cartilaginous substitute that mimics native tissue[8].

3D printing thrives in cartilage TE[9,10]. Extrusion-based bioprinting (EBB) uses a printing needle and Computer-Aided Design to deposit cellularized bioink onto support[11]. The bioink must be biocompatible and biodegradable, encouraging 3D cell differentiation[12]. Bio-extrusion produces large-volume pieces and stratified products, such as cartilaginous constructs, at a printing temperature compatible with living cells[13]. EBB generates a neo-tissue with physical and biochemical properties close to native tissue, making it a promising new cartilage defect repair method. The layer-by-layer construction allows the deposit of bioinks, growth factors, and cell types to mimic hyaline cartilage[14,15]. Nowadays, most EBB experiments aim to use triphasic stratified 3D-printed constructs to recreate three cartilaginous layers of the osteochondral interface[16-19]. Concerning cell sources, chondrocytes rapidly dedifferentiate and synthesize less ECM in 2D cell culture[20,21]. Mesenchymal stromal cells (MSCs) are promising candidates due to their high proliferation and chondrogenic properties. MSCs derived from bone marrow are the gold standard (BM-MSCs). The cellular density of MSCs used in cartilage 3D printing is high (>10M cells/mL), which is controversial for cartilage TE. Previous research has shown that a low cell density of 1M cells/mL more accurately represents cell repartition in native cartilage[22].

The most common bioinks for extrusion-based 3D printing are hydrogels made of natural biomaterials such as alginate, gelatin, type I collagen, hyaluronic acid, nanocellulose, or chitin[12]. They have numerous advantages because they are biocompatible, biodegradable, and cell-adhesive. However, hydrogels have poor mechanical strength and stability. Previous research used a patented bioink for 3D printing skin[23] to regenerate cartilage[22]. This bioink contained three cartilage tissue engineering components: alginate, gelatin, and fibrinogen. Gelatin hydrogels are non-immunogenic and biocompatible[24]. Gelatin-based hydrogels stimulate chondrogenic gene expression and protein synthesis in MSCs *in vitro* [25]. Because of its low stability, it necessitates gelation or biomaterial association; it is found in the cell walls of brown algae. Alginate is biocompatible, biodegradable, and has low cytotoxic potential[26]. Forming an "egg-box" structure[27] with a $CaCl_2$ solution gives the biomaterial a stable and compact 3D network while maintaining the chondrogenic phenotype[28-30]. Alginate and gelatin improve the biochemical and mechanical properties of the construct[31,32]. To stabilize the final construct, we added fibrin as a third component[22,23,33]. Thrombin converts fibrinogen into blood-clotting fibrin. Because of its reactivity with thrombin, fibrinogen can be added to bioink in 3D printing to include fibrin post-printing and improve stability[34]. Fibrin in gelatin-based bioink creates a more reticulated 3D network, retaining more cells in the printed substitutes and favoring the round morphology of chondrocytes[35].

According to our findings, human (h) BM-MSCs seeded in alginate, gelatin, and fibrinogen-based bioink can survive *in vitro* for 56 days. The printed constructs were homogenous with type II collagen and proteoglycan synthesis on D56[22]. The patented bioink, initially developed for skin bioprinting[23], requires a chondrogenic factor to produce a stratified construct that resembles native cartilage. This study incorporates a fourth natural biomaterial, type I collagen, into the bioink and modifies its concentration to recreate better specific hyaline cartilage layers, a challenge in cartilage TE. Unfortunately, exogenous type II collagen, naturally present in the cartilaginous matrix, may be immunogenic[36] and even arthritogenic in rodents[37] and monkeys[38]. In contrast, type I collagen has lower immunogenicity and is already used in the biomedical field[39], especially for cartilage engineering.

In an alginate-based hydrogel, type I collagen increased mechanical strength, cell adhesion, proliferation, survival, and chondrogenic gene expression[29]. The concentrations of collagen in hydrogel range from 0.03 to 3.00 mg/mL[40-42]. Some papers[43,44] use 10 or 40 mg/mL [**Supplementary Data 1**]. This work stayed within the parameters. The effect of gelatin, fibrinogen, and alginate-based bioink enriched or not with various type I collagen concentrations on the viability and chondrogenic potential of embedded MSCs, as well as their matrix synthesis in TE constructs to make specific cartilaginous layers of hyaline cartilage tissue *in vitro,* was thus investigated.

2. Methods

2.1. Isolation and expansion of human bone mesenchymal stromal cells

Bone marrows of three hip OA patients were isolated during arthroplasty. After informed consent from all study participants, the Bioethics Committee and our authorization (DC 2019-3387, authorized 2019, January 14th) approved the study. Biopsies were performed on two women (75 & 81 y.o.) and a man (77 y.o.). After anonymization, bone marrow samples were placed in 1 ml of phosphate-buffered saline (PBS, D8537, Sigma) with 625 UI/ml heparin. After dilution in 30 ml PBS, nucleated cells were collected by centrifugation at 400 g for 5 min. The cells were seeded into Petri dishes (90 mm diameter) at 4 x 10^6 cells/dish for monolayer expansion in Dulbecco's modified Eagle medium (DMEM-LG, 21885-025, Gibco) with low glucose (1 g/L) supplemented with 10% fetal bovine serum (FBS, P30-3306, Pan Biotech), 1% glutamine (35050-038, Gibco), 1% penicillin-streptomycin (15140-122, Gibco), and 1 ng/ml basic Fibroblast Growth Factor (bFGF, 130-093-837, Miltenyi France). Cells were incubated in a humidified atmosphere with 21% O_2 and 5% CO_2 incubated cells at 37°C. Twice-weekly culture medium changes were made.

Confluent (80%) MSCs were trypsinized using 0.05% trypsin-EDTA (25300-062, Gibco) and plated at 0.5 x 10^6 cells/dish density, then cultured from P0 to P3. In P3, before seeding in the bioink, the medium is changed for a chondrogenic pre-differentiation medium made of DMEM (DMEM-HG, 41965-039, Gibco), with high glucose (4.5 g/L) supplemented with 10% FBS, 1% glutamine, 1% penicillin-streptomycin, 110 µg/ml sodium pyruvate (11360-39, Gibco) and chondrogenic supplements: 40 µg/ml proline (P5607, Sigma), 50 µg/ml L-ascorbic-acid-2-phosphate (A8960, Sigma), and 10^{-7} M dexamethasone (D2915, Sigma) with 1 ng/mL of bFGF (130-093-837, Miltenyi France). P3 offers the best compromise between cell purity (>90%) and acquiring a sufficient cell number while maintaining excellent differentiation potentialities.

2.2. Bioink formulation

The authors created our lab-safe 3D printer. A push pump and heating patch keep the bio-extrusion system at 28°C. Repetier Host Software (Hot-World GmbH & Co. KG Knickelsdorf 4247877 Willich, Germany) monitors the printer and creates the construct printing pattern. The constructs were rectangular with a length of 1 cm, a width of 1 cm, and a thickness of 4 mm to deposit 4 layers. The bioink was formulated at 37°C with 1 percent (w/v) very low viscosity alginate (molecular weight: 216.121 g/mol, A18565, Alfa Aesar), 10% bovine gelatin (G1890, Sigma-Aldrich), and 2% fibrinogen (F8630, Sigma). Alginate was reconstituted in sodium chloride (NaCl 0.9 percent, 64812, Versol), and fibrinogen was diluted in cell culture media. Both solutions were placed at 37°C the day before printing for best dissolution and then filtered on a 0,22µm filters in accordance with the manufacturer's recommendations. The gelatin powder is already sterile; thus, it was weighted and diluted in a sterile environment, then also placed at 37°C overnight for best dissolution.

We added different amounts of soluble type I collagen (500060635, Viscofan) to bioink to test its effect. Thus, 0.0, 0.5, 1.0, and 5.0 mg of collagen per 8 ml were tested and coded as (a) Col0, (b) Col0.5, (c) Col1, and (d) Col5. The different quantities were chosen according to the Literature [43,44]. While reconstituting alginate with NaCl, sterile, soluble type I collagen was added to make 2 ml. The variation of each bioink rheology was too small to affect printability (**Supplementary Data 2**).

The constructs were printed layer-by-layer, following the design mentioned previously. The Petri dishes (430167, Dutscher) containing the newly printed constructs are filled with 20 ml of the gelation solution composed of 4% $CaCl_2$ (w/v) and 25 U/mL of thrombin (T4648, Sigma). The gelation of the construct takes 1 hour at 37°C under stirring (**Supplementary Data 3**). The substitutes were rinsed with a PBS solution and cultured for 28 or 56 days before harvest and evaluation. The culture medium was changed twice per week. For every bioink, the constructs were divided into two separate groups and cultured in a non-chondrogenic medium containing 1% glutamine, 1% penicillin-streptomycin,

110 µg/ml sodium pyruvate (11360-39, Gibco), 1mM $CaCl_2$, and chondrogenic supplements: 40 µg/ml proline (P5607, Sigma), 50 µg/ml L-ascorbic-acid-2-phosphate (A8960, Sigma), and 10^{-7} M dexamethasone (D2915, Sigma). 1% ITS (354352, Corning) was added in the control media, while ITS 1% and 10 ng/ml TGF-β1 (Miltenyi) were added to the chondrogenic medium.

2.3. Viability assays

We measured the supernatant lactate dehydrogenase (LDH) activity at D28 and D56 to determine cell viability in the 3D-printed constructs. The measure was made with a kit (Cytotoxicity Detection Kit^{PLUS}, Roche). For each concentration and condition tested in construct culture wells, 100 µL of supernatant was sampled. LDH activity was measured per the manufacturer's instructions. Spectrophotometers measured absorbance at 340 nm at each time point (Multiskan Ex, Thermo Labsystems). In each condition, a construct was sacrificed to set the maximum LDH release for the 100% cellular death threshold by adding Triton (2%) in the well, and an acellular gel was used for the 0% threshold. The value was reported to that threshold for each well and withdrawn from 100 to calculate the cell survival rate. Three patients had cell survival measured for three constructs per condition (n = 9).

2.4. Macroscopic observation

Before analysis, we took macroscopic images of the constructs at the experiment's start (**Supplementary Data 3**) and end (D56). A ruler calculates the scale of the photo on a flat, sterile surface. ImageJ calculated the total surface area (n = 9). TGF-β1-treated products are compared to ITS constructs of the same condition. TGF-β1/ITS shrinking ratios are computed for each bioink.

2.5. Gene expression analysis by quantitative real-time PCR

3D-bioprinted cartilages were frozen at -80°C after 28 or 56 days of maturation until analysis. β-mercaptoethanol-containing lysis buffer was digested for 10 minutes. The manufacturer's instructions were followed to purify the lysate on the purification column (QIAshredder, 79656, Qiagen). RNeasy Mini Kits isolated total mRNA (Qiagen). The Omniscript RT Kit reverse-transcribed 200 ng of RNA into cDNA (Qiagen). According to Qiagen's instructions, QuantiTectTM SYBR Green PCR was used for qRT-PCR. A standard curve was created from purified PCR products for each gene (10^{-3} to 10^{-6} ng/µL) to determine relative quantification. Aggrecan (*ACAN*), Type 2 Collagen (*COL2A1*), its isoform IIB (*COLIIB*), SRY-Box Transcription Factor 9 (*SOX9*), Type 1 Collagen (*COL1A1*), Versican (*VCAN*), RUNT-related transcription factor 2 (*RUNX2*), Cartilage Oligomeric Matrix Protein (*COMP*), Alkaline Phosphatase (*ALPL*), Osteocalcin (*BGLAP*), Matrix Metallopeptidase 13 (*MMP13*), and Type 10 Collagen (*COL10A1*) gene expression levels were normalized to *RPS29*. This constitutive gene is expressed relatively consistently, regardless of experimental conditions. **Supplementary Data 4** shows sequences and product sizes. The measures were repeated on three patients in triplicate biological samples for each gene (n=9).

2.6. Biochemical assay of GlysosAminoGlycan content

Colorimetric quantification measured GAG content [45]. After 28 or 56 days of maturation, 3D-printed constructs were dried overnight and weighed. The constructs were digested overnight at 60°C in 200 µL buffer and 10 µL papain solution (60 µg / 10 µL, P4762, Sigma). Then, 10 µL of 0.22 mol/L monoiodoacetic acid stopped the reaction (MIA, Merck). For each sample, 20 µL of supernatant was placed in a 96-well plate, to which 250 µL of 9.2 x 10^{-5} mol 1,9-dimethyl methylene blue (DMB, 23481-50-7, Polysciences) was added to form a soluble GAG-DMB complex. A standard curve of shark cartilage chondroitin-6-sulfate from 0 to 100 µg/mL was used to calculate GAG content (C6S, C4384, Sigma). A 525-nm spectrophotometer read the 96-well plate. The samples' initial dry weight normalized the GAG content (mg). Acellular constructs were dosed and subtracted from the GAG content of the cellularized hydrogels. The measures were repeated on three constructs for all three patients (n=9).

2.7. Histological analysis of cartilaginous printed constructs

Histology examined extracellular matrix synthesis 28 or 56 days after printing. The constructs were fixed in a buffer with 4% paraformaldehyde, 10 mM $CaCl_2$, and 0.1 M sodium cacodylate (pH 7.4) for 24 h at room temperature, then washed at 4°C in a solution with 50 mM $BaCl_2$. The constructs were dehydrated in ethanol, embedded in paraffin, and cut into 5 µm cross sections. Hematoxylin-Erythrosin-Saffron (HES) staining revealed the constructs' cell morphology and matrix organization. Alcian blue stained 3D constructs' sulfated glycosaminoglycans (GAGs) (AB, pH 1.3). Alizarin red (AR,

pH 4.2) stained calcium deposits. Light microscopy (DMD 108, Leica) was used to record the stained slides of three constructs per patient (n = 9). One photo per condition was selected.

2.8. Immunohistochemical staining of cartilaginous printed constructs

Immunohistochemistry was used to analyze extracellular matrix synthesis 28 or 56 days after printing. Type II collagen immunostaining with type II collagen antibodies (6B3, MS-306-R7, Labvision) at a dilution of 1% was used to assess MSC chondrogenic differentiation and matrix synthesis in hydrogels. Deparaffinized 5µm slides were treated with pepsin (0.4% w/v in 0.01 M HCl, pH 2.0) for 30 min at room temperature. The samples were washed and incubated with a hydrogen peroxide-blocking solution to block endogenous peroxidase. Stopping unspecific epitopes requires 2% BSA. Primary and secondary antibodies incubated the samples. DAB (LSAB + HRP kit, Dako) in the substrate-chromogen solution causes a brown residue. Sections were counterstained with hematoxylin and then mounted with resin. Light microscopy recorded stained slides (DMD 108, Leica®). Nine constructs were photographed.

2.9. Densitometry analysis of the constructs

ImageJ was used to analyze semi-quantitatively AB, AR, and type II collagen immunohistochemistry images. After measuring the constructs' total size, hue, and saturation, they were isolated from the positively stained area. The measures were repeated on three slides per patient (n=9).

2.10. Statistical analysis

Three patients per condition were tested in biological triplicate (LDH assay, macroscopic observation, gene expression, histological, immunohistochemical, and biochemical assay). TGF-β1 to control is the shrinking ratio for each situation (n = 9) vs. ITS. For gene expression standardization, results were expressed as a ratio of the mRNA level of each gene of interest over the *RPS29* gene in every bioink and presented as mean + standard error to the mean (SEM). For all other experiments, a one-way ANOVA comparison test was used to determine significance, followed by Tukey's post-hoc test for multiple comparisons to compare TGF-β1 with our control condition ITS, then the effect of the four bioinks and time. GraphPad Prism® performed the statistical analysis.

3. Results

3.1. Effect of collagen addition on embedded cells viability during chondrogenesis

LDH dosages were measured after D28 or D56 of *in vitro* maturation in ITS or TGF-β1 conditions for the four bioinks to determine the effect of type I collagen on cell viability. **Figure 1** shows the results. LDH dosage viability ranged from 91-95 percent in all tested conditions and for the four bioinks, proving that the global printing process and bioink constitution did not affect cell viability.

3.2. Macroscopic effect of the TGF-β1 chondrogenic induction on the different constructs printed using the four bioinks of interest

At the end point of our experiment (D56), the bio-extruded constructs were subjected to a macroscopic observation. The pink coloration was due to the cell culture medium (**Figure 2A**). Sectioned in half for analysis, those constructs were smaller, rounder, denser, and harder to cut. The shrinkage ratio was calculated as TGF-β1 /ITS (**Figure 2B**). Col0.5 had a 1.3-fold higher shrinking ratio than Col0, indicating higher MEC synthesis. Col1 and Col5 inks differed 0.8 and 0.7-fold from the control ink (ITS, without TGF-β1).

3.3. Gene expressions in the 3D printed constructs

At D28, TGF-β1 induced chondrogenic differentiation in the embedded cells in bio-extruded constructs in all bioinks, but Col5 is less so (**Figure 3).** TGF-β1 supported chondrogenic differentiation by generating chondrogenic markers like *COL2A1, COL2B, COL10, ACAN, SOX9*, and *COMP*. Otherwise, *RUNX2* and *COL1A1* were also upregulated. Interestingly, *VCAN, ALPL*, and *BGLAP* levels remained low.

At D28, Col0.5 specifically increased *COL2A1, COL2B, COL10A1*, and *COMP* by 1.8 and 2.6-fold, respectively, compared to Col0. MSCs from all our end-stage OA patients overexpressed *COL10A1. COL1A1* levels were slightly higher but positively correlated with chondrogenic markers. Col1 and Col5 did not increase chondrogenic markers. Col5 also decreased *ACAN* expression and overexpressed *BGLAP* (2.7-fold), *RUNX2* (1.4-fold), and *MMP13* (238.0-fold), favoring osteogenicity. All gene expression drops to the basal level at D56.

3.4. Biochemical analysis for GAGs content

After D28 and D56 of *in vitro* culture, mature GAGs were quantified. **Figure 4** shows the results. In the chondrogenic condition, Col0 and Col0.5 bioinks synthesized significantly more GAGs in their ECMs than in the control condition (ITS). TGF-β1 increased synthesis in Col0.5 by 1.7-fold on D28 compared to *Col0* but decreased synthesis at D56 (1.7-fold) compared to *Col0*. Col1 and Col5 bio-inks had folds of 0.5 and 0.7 on D28 and 0.3 and 0.4 on D56 compared to Col0. Despite maturation, TGF-β1 did not promote GAG synthesis in those two inks. The Col0.5 bioink constructs' GAG synthesis decreased from D28 to D56.

3.5. Histological and immunostaining analysis

The bio-extruded constructs showed that all four bioinks retained a dense, homogeneous global structure after D28 or D56, regardless of the four initially printed layers. HES staining showed homogeneous cell distribution within constructs with no embedded cell mortality (data not shown). Bio-extruded constructs in ITS conditions showed weak extracellular matrix synthesis in proteoglycans and collagen. TGF-β1 increased Alcian blue-stained GAG in all four bioinks at D56 (**Figures 5A and 5B**). After D56, the positively stained areas are higher than 30%, with Col0 (47%), Col1 (50%), and Col0.5 (55%).

Concerning Col0.5 and Col1, maturation time significantly increased proteoglycan synthesis, but not for Col0 and Col5 bioinks. D28 showed no type II collagen synthesis by specific staining (**Figures 5C and 5D**). After D56, immunostaining showed a positive effect of TGF-β1 for the Col0 (19%), Col0.5 (34%), and Col1 (27%) bioinks, but no type II collagen synthesis in the Col5 bioink. Col0.5 bioink produced 1.8-fold more intense brown staining than Col0 bioink, indicating that this quantity of type I collagen affected type II collagen synthesis in bio-extruded constructs. Col1 bioink had similar type II collagen staining to Col0. Col5 synthesized 5% less than its ITS controls. The edges of the constructs contain higher proteoglycan and type II collagen synthesis, while the central area was less stained in all conditions, likely due to the gradient of media and nutrient diffusion. The constructs' two major hyalin MEC components were precisely co-located in histology slides.

Alizarin red, specifically stains construct calcium deposition. At D28, the ITS condition had the highest red staining on the construct edges (**Figures 5E and 5F**). After D56, TGF-β1 maintained less than 12% of the total calcified area in constructs printed with Col0, Col0.5, or Col1 bioinks, compared to ITS conditions. At D56, the Col5 constructs had five times more calcifications (39%) than the bioink without collagen (7%) in the chondrogenic environment. Unlike the edge staining of the ITS conditions, the latter had homogenous staining in the constructs' center areas.

4. Discussion

In this study, we aimed to use extrusion-based bioprinting of alginate, gelatin, and fibrinogen-based bioinks to produce functionalized cartilaginous constructs. We first confirmed that the global bioprinting process, as well as the collagen addition in our bioink, do not have a deleterious effect on the embedded cells' viability. Then, we showed that MSCs seeded in all tested bioinks and cultured in a TGF-β1-enriched medium differentiated into chondrogenic cells. Maturation time impacted both gene expression and matrix synthesis. While gene expression is higher after 28 days, a dense ECM in constructs requires 56 days of *in vitro* growth. Our work is in accordance with many studies already showing that BM-MSC-seeded bio-extruded functionalized constructs are successful in cartilage tissue engineering[46]. The limitation of classical tissue engineering methods that use homogenous scaffolds is that they make replicating and constructing the zonal organization harder. In contrast, new 3D printing processes make layer regeneration easier. It is well known that cell density, ink composition, and viscosity are all key factors that affect EBB printing. Furthermore, the construct's final ink gelation and reticulation directly impact the cells' environment and, thus, their ability to differentiate into the chondrogenic pathway[47].

Biocompatibility, biodegradability, and cartilaginous-like structure make natural biomaterials ideal for cartilage TE. In this work, we based this composition on our previous work comparing three different bioinks. According to those previous results, we bioextruded a bioink composed of alginate, gelatin, and fibrinogen[23,48]. Gelatin can be methacrylated[49-51] or combined with other natural components to improve its stability. It is often used in tissue engineering for its biocompatibility, biodegradability, and easy gelation[26,52]. Its concentration affects bio-constructs' 3D network and encapsulated cell chondrogenesis[53]. Fibrin is formed by the reaction of fibrinogen and thrombin. Due to its fiber orientation, it promotes cell self-organization[48]. Fibrinogen concentration affects bioink viscosity, reticulation[17], cell growth, and division[54].

This study first showed that our extrusion-based bioprinting process could produce a 4 mm thick construct in a layer-by-layer process. Literature has already demonstrated that conical needles, biocompatible pressure, and extrusion speed ensured cell viability in the constructs[22]. Furthermore, collagen is known to improve cell adhesion and viability in biomaterials[29,55]. Our results are by those statements, as our printing method, bioink composition, and cell conditions do not affect cell viability, which stays excellent until 56 days of maturation. We obtained an overall survival rate above 90% in all tested conditions. Furthermore, similarly to what is shown in the literature, the addition of soluble type I collagen in our bioink does not affect the construct's global printing process[22,56]. We also demonstrated that our functionalized constructs in chondrogenic differentiation media (TGF-β1) support MSCs' chondrogenic differentiation. TGF-β1 promoted chondrogenesis in all four bioinks, and resulting ECM synthesis shrinks constructs macroscopically. Histological and immunohistochemical staining of our constructs confirms the matrix's proteoglycans and type II collagen contents in chondrogenic conditions.

Literature shows that RGD peptides on collagen fibers, an ECM protein, improve cell adhesion and chondrogenesis[57]. We found that adding 0.5mg of collagen I to our bioink increases explicitly gene expression of cartilaginous markers like *COL2A1, COL2B*, and *COMP*, which are correlated with the maintenance of the chondrogenic phenotype. The beneficial effect of type I collagen on cells' chondrogenesis and gene expression of those specific genes was already demonstrated by Yang et al.[29]. This specific collagen quantity also increases the matrix's proteoglycans and type II collagen synthesis, creating a dense, rich, hyaline-like ECM in the constructs. On the contrary, a higher type I collagen quantity increases hypertrophic/calcified markers like *MMP13*, *RUNX2*, and *BGLAP*[41]. Calcium deposition in the matrix is also higher. Many studies have shown that matrix reticulation is critical in maintaining the chondrogenic phenotype[47]. The final hydrogel reticulation in the construct containing 5mg of collagen may be responsible for the construct hypertrophy. Our results suggest that collagen type-I enriched bio-inks can dose-dependently promote either a chondrogenic or hypertrophic/calcified phenotype, potentially providing an excellent layer-by-layer construct containing both chondral and osteochondral structures with a unique differentiation medium.

In conclusion, the Col0.5 bioink is a promising candidate to reproduce the superficial layers of hyaline cartilage without affecting its rheological properties. The resulting layer is a proteoglycan- and type II collagen-rich extracellular matrix with a more hyaline-like MSC profile and a lower hypertrophic/osteogenic profile (*BGLAP, RUNX2*, and *MMP13*). In contrast, Col5 bioink can mimic the hypertrophic/calcified area of native cartilage. These bioinks could help us to 3D print a stratified construct to repair articular cartilage.

Author's-contribution

OM, CH, and EJC were involved in the cell culture, 3D printing process, and histological, biochemical, and statistical analyses. OM contributed to the manuscript preparation. LGr, DM, LGa, DL, and CM were involved in the intellectual contribution and editing of the manuscript. CH, PG, and AP contributed to the synthesis and editing of the manuscript. All authors have contributed substantially to the study's conception and design. All authors have revised it critically for important intellectual content. All authors have given final approval of this present version.

Funding

This work has been funded by

- ANR-DGA Bloc print Direction Générale des Armées (DGA), Grant/Award Number: ANR-16-ASTR-0021,
- CPER IT2MP (Contrat Plan État Région, Innovations Technologiques, Modélisation & Médecine Personnalisée) and FEDER (Fonds européen de développement régional)
- Fondation de l'Avenir pour la Recherche Médicale Appliquée, Grant/Award Number: AP-RM-16-042"
- Université de Lorraine - Région Alsace-Champagne-Ardennes-Lorraine 2016, Grant/Award Number: AAP-002-037
- Océane MESSAOUDI was supported by the Fondation pour la Recherche Médicale (FRM), Grant/Award Number ECO201906008942.

Acknowledgments

We thank the hospital staff of Chirurgie Orthopédique Traumatologique & Arthroscopique and Centre Emile GALLÉ, CHRU Nancy, for retrieving and providing the biological samples. We also thank Magali DETZ (Technician) for her help in the histology department.

Declaration of INTEREST

The authors declare that they have no known competing financial interests or personal relationships that could have appeared to influence the work reported in this paper.

Sharing of Materials

Authors will honor any reasonable request for materials, methods, or data necessary to reproduce or validate the research

Abbreviations

2D: Two-Dimensional
3D: Three-Dimensional
AB: Alcian blue
ACAN: Aggrecan (gene)
ANOVA: Analysis of variance
AR: Alizarin red
bFGF: basic Fibroblast Growth Factor
BGLAP: Osteocalcin (gene)
CAD: Computer-Aided Design
CO_2: Carbon Dioxide
COL10A1: Collagen type X alpha one chain (gene)
COL2A: Collagen type II alpha 1 chain (gene)
COMP: Cartilage Oligomeric Matrix Protein (gene)
DMB: 1,9-Dimethyl Methylene blue
DMEM: Dulbecco's Modified Eagle Medium
DO: Absorbance
EBB: Extrusion-Based Bioprinting
ECM: Extracellular Matrix
FBS: Fetal Bovine Serum
GAG: GlycosAminoGlycan
HES: Hematoxylin Erythrosin Saffron
ITS: Insulin-Transferrin-Selenium
LDH: Lactate DeHydrogenase
MIA: Mono Iodoacetic Acid
MMP13: Matrix Metallopeptidase 13 (gene)
MSCs: Mesenchymal Stromal Cells
OSX: Osterix (gene)
PBS: Phosphate-Buffered Saline
qRT-PCR: Quantitative reverse transcription polymerase chain reaction
RNA: Ribonucleic acid
RPS29: Ribosomal protein S29 (gene)
SOX9: Sex-determining region-related HMG-box9 (gene)
TE: Tissue engineering

Figures legends

Figure 1: **Cell viability was evaluated by supernatant LDH dosage measures at D28 and D56 for the *Col0*, *Col0.5*, *Col1,* and *Col5* bioinks in ITS and TGF-β1 conditions.** Data are shown as mean + SEM. (n=9). One-way ANOVA did not show significant differences between each bioink and each situation.

Figure 2: **Macroscopic observation of the cartilaginous substitutes at D56** (A) Macroscopic images of cell-seeded bio-extruded constructs using *Col0*, *Col0.5*, *Col1*, and *Col5* bioinks in both ITS (top line) and TGF-β1 (bottom line) conditions on D56. (B) The shrinking ratio between TGF-β1 and ITS conditions for every bioink. Data are shown as mean + SEM. Measures were done in triplicates. Every bioink was compared to the three others using a one-way ANOVA, followed by a Tukey's post hoc test, * $p < 0.05$, ** $p < 0.01$, *** $p < 0.001$.

Figure 3: **Influence of growth factor TGF-β1, time, and bioink composition on gene expressions in bioprinted cartilage constructs on D28 and D56.** Chondrogenic, hypertrophic, and fibrotic marker expressions were investigated using real-time qPCR. In the first step, comparisons for each condition were performed versus their respective control condition (ITS alone) with one-way ANOVA followed by Tukey's test. Data are presented as the mean + SEM. ∗$p < 0.05$, ∗∗$p < 0.01$, and ∗∗∗ $p < 0.001$ vs. ITS. A one-way ANOVA, followed by Tukey's post hoc test, was performed to assess the influence of time in each respective condition. # $p < 0.05$, ## $p < 0.01$, and ### $p < 0.001$. Lastly, the effect of the bioink composition was assessed between each composition within a given condition (time point and growth factor). § $p < 0.05$, §§ $p < 0.01$, and §§§ $p < 0.001$; ns: not significant.

Figure 4: **Glycosaminoglycans (GAGs) assay in the extruded constructs after 56 days of maturation under the effect of TGF-β1 or in the ITS condition normalized by using acellular constructs as control.** The results are expressed in micrograms of GAG per milligram of the dry weight of the final constructs. The numbers are shown in mean + SEM for each condition (n=9). For every bioink, TGF-β1 was compared to the ITS control using a one-way ANOVA, followed by a Tukey's post hoc test, * $p < 0.05$, ** $p < 0.01$, *** $p < 0.001$. Every bioink was compared to the three others using a one-way ANOVA, # $p < 0.05$, ## $p < 0.01$, ### $p < 0.001$, ns=not significative, and the effect of the maturation time was evaluated using 1 Factor ANOVA.

Figure 5: **Histological and immunohistochemical analyses of 3D-printed constructs seeded with BM-MSCs using either *Col0*, *Col0.5*, *Col1,* or *Col5* bioink in ITS and TGF-β1 on D28 and D56 post-printing**. The proteoglycans synthesized were stained using Alcian blue staining (A), the type II collagen was observed using immunohistochemistry (brown staining) (C), and calcified deposition was stained using Alizarin red (E). Quantitative analyses of the histological and immunohistological staining with Alcian blue (B), immunohistochemical evidence of type II collagen (D), and calcifications (F) in the bio-extruded constructs were performed with ImageJ. The results are expressed as the percentage mean + SEM of the stained area (n=9). For every bioink, TGF-β1 was compared to the ITS control using a one-way ANOVA, * $p < 0.05$, ** $p < 0.01$, *** $p < 0.001$, and the effect of the maturation time was evaluated using one-way ANOVA, # $p < 0.05$, ## $p < 0.01$, ### $p < 0.001$. Every bioink was compared to the three others using a one-way ANOVA followed by Tukey's test, § $p < 0.05$, §§ $p < 0.01$, §§§ $p < 0.001$, ns = no significant difference.

References

1. Neogi T, Zhang Y. Epidemiology of osteoarthritis. Rheumatic Diseases Clinics of North America 2013;39(1):1-19, doi:10.1016/j.rdc.2012.10.004

2. Vina ER, Kwoh CK. Epidemiology of osteoarthritis: literature update. Current Opinion in Rheumatology 2018;30(2):160-167, doi:10.1097/BOR.0000000000000479

3. Dieppe PA, Lohmander LS. Pathogenesis and management of pain in osteoarthritis. Lancet (London, England) 2005;365(9463):965-973, doi:10.1016/S0140-6736(05)71086-2

4. Trouvin A-P, Perrot S. Pain in osteoarthritis. Implications for optimal management. Joint Bone Spine 2018;85(4):429-434, doi:10.1016/j.jbspin.2017.08.002

5. Matthews JR, Brutico JM, Abraham DT, et al. Differences in Clinical and Functional Outcomes Between Osteochondral Allograft Transplantation and Autologous Chondrocyte Implantation for the Treatment of Focal Articular Cartilage Defects. Orthopaedic Journal of Sports Medicine 2022;10(2):23259671211058425, doi:10.1177/23259671211058425

6. Solheim E, J H, T S, et al. Randomized Study of Long-term (15-17 Years) Outcome After Microfracture Versus Mosaicplasty in Knee Articular Cartilage Defects. The American journal of sports medicine 2018;46(4), doi:10.1177/0363546517745281

7. Brittberg M. Autologous chondrocyte implantation—Technique and long-term follow-up. Injury 2008;39(1, Supplement):40-49, doi:10.1016/j.injury.2008.01.040

8. Guo X, Ma Y, Min Y, et al. Progress and prospect of technical and regulatory challenges on tissue-engineered cartilage as therapeutic combination product. Bioactive Materials 2022;20(501-518, doi:10.1016/j.bioactmat.2022.06.015

9. Xie Z, Gao M, Lobo A, et al. 3D Bioprinting in Tissue Engineering for Medical Applications: The Classic and the Hybrid. Polymers 2020;12(doi:10.3390/polym12081717

10. Yilmaz B, Tahmasebifar A, Baran ET. Bioprinting Technologies in Tissue Engineering. Advances in Biochemical Engineering/Biotechnology 2019, doi:10.1007/10_2019_108

11. Ozbolat IT, Hospodiuk M. Current advances and future perspectives in extrusion-based bioprinting. Biomaterials 2016;76(321-343, doi:10.1016/j.biomaterials.2015.10.076

12. Gungor-Ozkerim PS, Inci I, Zhang YS, et al. Bioinks for 3D bioprinting: an overview. Biomaterials Science 2018;6(5):915-946, doi:10.1039/c7bm00765e

13. Derakhshanfar S, Mbeleck R, Xu K, et al. 3D bioprinting for biomedical devices and tissue engineering: A review of recent trends and advances. Bioactive Materials 2018;3(2):144-156, doi:10.1016/j.bioactmat.2017.11.008

14. Shim J-H, Jang K-M, Hahn SK, et al. Three-dimensional bioprinting of multilayered constructs containing human mesenchymal stromal cells for osteochondral tissue regeneration in the rabbit knee joint. Biofabrication 2016;8(1):014102, doi:10.1088/1758-5090/8/1/014102

15. Barthold JE, McCreery KP, Martinez J, et al. Particulate ECM biomaterial ink is 3D printed and naturally crosslinked to form structurally-layered and lubricated cartilage tissue mimics. Biofabrication 2022;14(2), doi:10.1088/1758-5090/ac584c

16. Li Z, Jia S, Xiong Z, et al. 3D-printed scaffolds with calcified layer for osteochondral tissue engineering. Journal of Bioscience and Bioengineering 2018;126(3):389-396, doi:10.1016/j.jbiosc.2018.03.014

17. Han Y, Lian M, Sun B, et al. Preparation of high precision multilayer scaffolds based on Melt Electro-Writing to repair cartilage injury. Theranostics 2020;10(22):10214-10230, doi:10.7150/thno.47909

18. Zhu M, He X, Xin C, et al. 3D printing of an integrated triphasic MBG-alginate scaffold with enhanced interface bonding for hard tissue applications. Journal of Materials Science Materials in Medicine 2020;31(12):113, doi:10.1007/s10856-020-06459-6

19. Qiao Z, Lian M, Han Y, et al. Bioinspired stratified electrowritten fiber-reinforced hydrogel constructs with layer-specific induction capacity for functional osteochondral regeneration. Biomaterials 2021;266(120385, doi:10.1016/j.biomaterials.2020.120385

20. Cournil-Henrionnet C, Huselstein C, Wang Y, et al. Phenotypic analysis of cell surface markers and gene expression of human mesenchymal stem cells and chondrocytes during monolayer expansion. Biorheology 2008;45(3-4):513-526, doi:10.3233/BIR-2008-0487

21. Izadifar Z, Chang T, Kulyk W, et al. Analyzing Biological Performance of 3D-Printed, Cell-Impregnated Hybrid Constructs for Cartilage Tissue Engineering. Tissue Engineering Part C, Methods 2016;22(3):173-188, doi:10.1089/ten.TEC.2015.0307

22. Henrionnet C, Pourchet L, Neybecker P, et al. Combining Innovative Bioink and Low Cell Density for the Production of 3D-Bioprinted Cartilage Substitutes: A Pilot Study. Stem Cells International 2020;2020(e2487072, doi:10.1155/2020/2487072

23. Pourchet LJ, Thepot A, Albouy M, et al. Human Skin 3D Bioprinting Using Scaffold-Free Approach. Advanced Healthcare Materials 2017;6(4), doi:10.1002/adhm.201601101

24. Lukin I, Erezuma I, Maeso L, et al. Progress in Gelatin as Biomaterial for Tissue Engineering. Pharmaceutics 2022;14(6):1177, doi:10.3390/pharmaceutics14061177

25. Salamon A, van Vlierberghe S, van Nieuwenhove I, et al. Gelatin-Based Hydrogels Promote Chondrogenic Differentiation of Human Adipose Tissue-Derived Mesenchymal Stem Cells In Vitro. Materials 2014;7(2):1342-1359, doi:10.3390/ma7021342

26. Rastogi P, Kandasubramanian B. Review of alginate-based hydrogel bioprinting for application in tissue engineering. Biofabrication 2019;11(4):042001, doi:10.1088/1758-5090/ab331e

27. Grant GT, Morris ER, Rees DA, et al. Biological interactions between polysaccharides and divalent cations: The egg-box model. FEBS Letters 1973;32(1):195-198, doi:10.1016/0014-5793(73)80770-7

28. Khalil S, Sun W. Bioprinting endothelial cells with alginate for 3D tissue constructs. Journal of Biomechanical Engineering 2009;131(11):111002, doi:10.1115/1.3128729

29. Yang X, Lu Z, Wu H, et al. Collagen-alginate as bioink for three-dimensional (3D) cell printing based cartilage tissue engineering. Materials Science & Engineering C, Materials for Biological Applications 2018;83(195-201, doi:10.1016/j.msec.2017.09.002

30. Chu Y, Huang L, Hao W, et al. Long-term stability, high strength, and 3D printable alginate hydrogel for cartilage tissue engineering application. Biomedical Materials (Bristol, England) 2021;16(6), doi:10.1088/1748-605X/ac2595

31. Schwarz S, Kuth S, Distler T, et al. 3D printing and characterization of human nasoseptal chondrocytes laden dual crosslinked oxidized alginate-gelatin hydrogels for cartilage repair approaches. Materials Science & Engineering C, Materials for Biological Applications 2020;116(111189, doi:10.1016/j.msec.2020.111189

32. Iranmanesh P, Gowdini M, Khademi A, et al. Bioprinting of three-dimensional scaffold based on alginate-gelatin as soft and hard tissue regeneration. Journal of Materials Research and Technology 2021;14(2853-2864, doi:10.1016/j.jmrt.2021.08.069

33. Rojas-Murillo JA, Simental-Mendía MA, Moncada-Saucedo NK, et al. Physical, Mechanical, and Biological Properties of Fibrin Scaffolds for Cartilage Repair. International Journal of Molecular Sciences 2022;23(17):9879, doi:10.3390/ijms23179879

34. Weisel JW. Fibrinogen and Fibrin. In: Advances in Protein Chemistry. Academic Press: 2005; pp. 247-299.

35. Wang ZH, Zhang J, Zhang Q, et al. Evaluation of bone matrix gelatin/fibrin glue and chitosan/gelatin composite scaffolds for cartilage tissue engineering. Genetics and molecular research: GMR 2016;15(3), doi:10.4238/gmr.15038431

36. Elango J, Zamora-Ledezma C, Ge B, et al. Paradoxical Duel Role of Collagen in Rheumatoid Arthritis: Cause of Inflammation and Treatment. Bioengineering (Basel, Switzerland) 2022;9(7):321, doi:10.3390/bioengineering9070321

37. Brand DD, Latham KA, Rosloniec EF. Collagen-induced arthritis. Nature Protocols 2007;2(5):1269-1275, doi:10.1038/nprot.2007.173

38. Yoo TJ, Kim SY, Stuart JM, et al. Induction of arthritis in monkeys by immunization with type II collagen. The Journal of Experimental Medicine 1988;168(2):777-782, doi:10.1084/jem.168.2.777

39. Zhang J, Elango J, Wang S, et al. Characterization of Immunogenicity Associated with the Biocompatibility of Type I Collagen from Tilapia Fish Skin. Polymers 2022;14(11):2300, doi:10.3390/polym14112300

40. Lee J, Yeo M, Kim W, et al. Development of a tannic acid cross-linking process for obtaining 3D porous cell-laden collagen structure. International Journal of Biological Macromolecules 2018;110(497-503, doi:10.1016/j.ijbiomac.2017.10.105

41. Kim YB, Lee H, Kim GH. Strategy to Achieve Highly Porous/Biocompatible Macroscale Cell Blocks, Using a Collagen/Genipin-bioink and an Optimal 3D Printing Process. ACS Applied Materials & Interfaces 2016;8(47):32230-32240, doi:10.1021/acsami.6b11669

42. Ren X, Wang F, Chen C, et al. Engineering zonal cartilage through bioprinting collagen type II hydrogel constructs with biomimetic chondrocyte density gradient. BMC musculoskeletal disorders 2016;17(301, doi:10.1186/s12891-016-1130-8

43. She Y, Fan Z, Wang L, et al. 3D Printed Biomimetic PCL Scaffold as Framework Interspersed With Collagen for Long Segment Tracheal Replacement. Frontiers in Cell and Developmental Biology 2021;9(629796, doi:10.3389/fcell.2021.629796

44. Lee C-F, Hsu Y-H, Lin Y-C, et al. 3D Printing of Collagen/Oligomeric Proanthocyanidin/Oxidized Hyaluronic Acid Composite Scaffolds for Articular Cartilage Repair. Polymers 2021;13(18):3123, doi:10.3390/polym13183123

45. Goldberg RL, Kolibas LM. An improved method for determining proteoglycans synthesized by chondrocytes in culture. Connective Tissue Research 1990;24(3-4):265-275, doi:10.3109/03008209009152154

46. Messaoudi O, Henrionnet C, Bourge K, et al. Stem Cells and Extrusion 3D Printing for Hyaline Cartilage Engineering. Cells 2021;10(1):2, doi:10.3390/cells10010002

47. Costantini M, Idaszek J, Szöke K, et al. 3D bioprinting of BM-MSCs-loaded ECM biomimetic hydrogels for in vitro neocartilage formation. Biofabrication 2016;8(3):035002, doi:10.1088/1758-5090/8/3/035002

48. Xu M, Wang X, Yan Y, et al. An cell-assembly derived physiological 3D model of the metabolic syndrome, based on adipose-derived stromal cells and a gelatin/alginate/fibrinogen matrix. Biomaterials 2010;31(14):3868-3877, doi:10.1016/j.biomaterials.2010.01.111

49. Lam T, Dehne T, Krüger JP, et al. Photopolymerizable gelatin and hyaluronic acid for stereolithographic 3D bioprinting of tissue-engineered cartilage. Journal of Biomedical Materials Research Part B, Applied Biomaterials 2019;107(8):2649-2657, doi:10.1002/jbm.b.34354

50. Gu L, Li T, Song X, et al. Preparation and characterization of methacrylated gelatin/bacterial cellulose composite hydrogels for cartilage tissue engineering. Regenerative Biomaterials 2020;7(2):195-202, doi:10.1093/rb/rbz050

51. Luo X, Liu Y, Pang J, et al. Thermo/photo dual-crosslinking chitosan-gelatin methacrylate hydrogel with controlled shrinking property for contraction fabrication. Carbohydrate Polymers 2020;236(116067, doi:10.1016/j.carbpol.2020.116067

52. Olate-Moya F, Arens L, Wilhelm M, et al. Chondroinductive Alginate-Based Hydrogels Having Graphene Oxide for 3D Printed Scaffold Fabrication. ACS Appl Mater Interfaces 2020;12(4):4343-4357, doi:10.1021/acsami.9b22062

53. Ewa-Choy YW, Pingguan-Murphy B, Abdul-Ghani NA, et al. Effect of alginate concentration on chondrogenesis of co-cultured human adipose-derived stem cells and nasal chondrocytes: a biological study. Biomaterials Research 2017;21(doi:10.1186/s40824-017-0105-7

54. Han W, Singh NK, Kim JJ, et al. Directed differential behaviors of multipotent adult stem cells from decellularized tissue/organ extracellular matrix bioinks. Biomaterials 2019;224(119496, doi:10.1016/j.biomaterials.2019.119496

55. Holmes B, Zhu W, Li J, et al. Development of Novel Three-Dimensional Printed Scaffolds for Osteochondral Regeneration. Tissue Engineering Part A 2015;21(1-2):403-415, doi:10.1089/ten.tea.2014.0138

56. Marques CF, Diogo GS, Pina S, et al. Collagen-based bioinks for hard tissue engineering applications: a comprehensive review. Journal of Materials Science Materials in Medicine 2019;30(3):32, doi:10.1007/s10856-019-6234-x

57. Bellis SL. Advantages of RGD peptides for directing cell association with biomaterials. Biomaterials 2011;32(18):4205-4210, doi:10.1016/j.biomaterials.2011.02.029

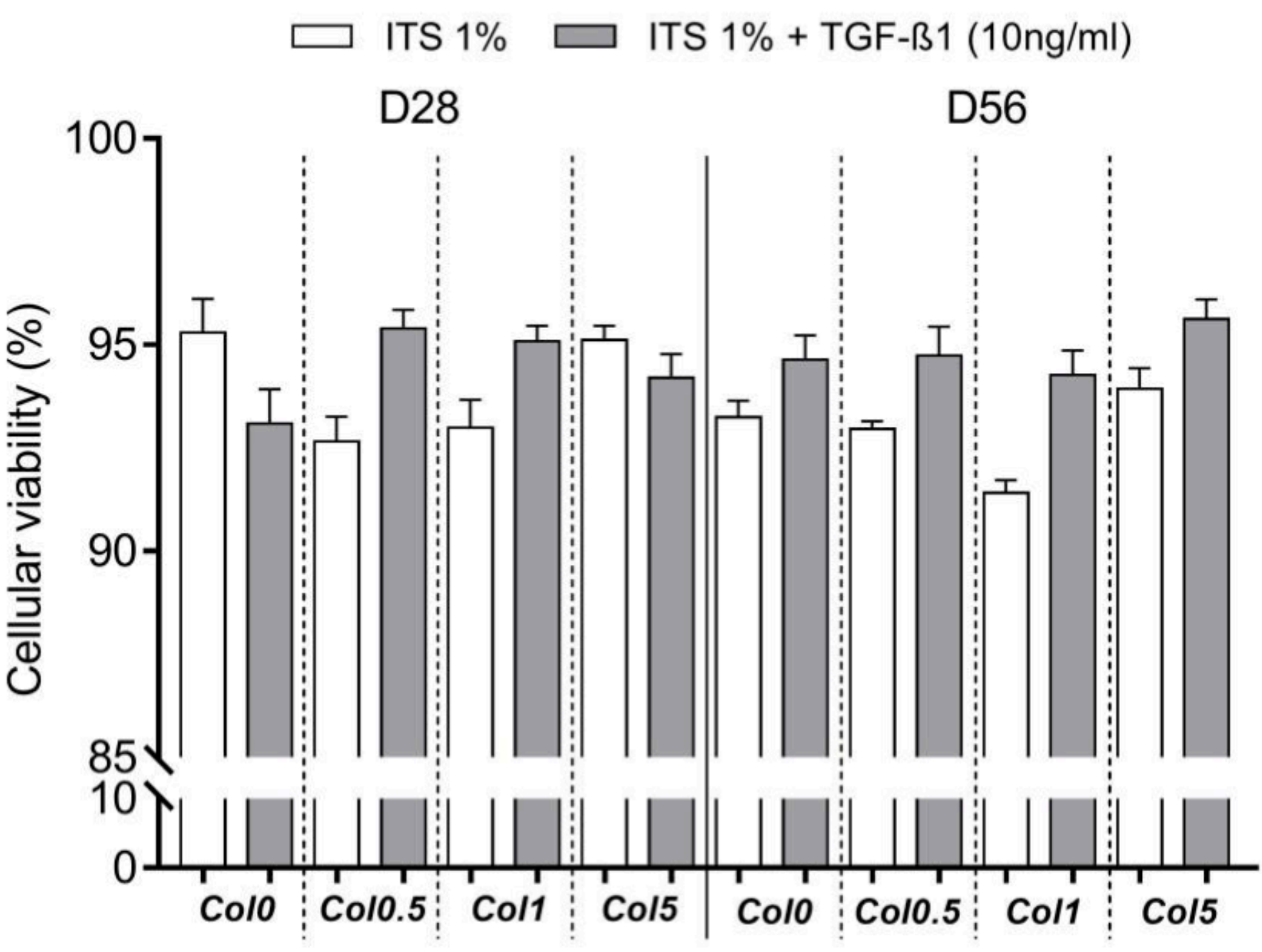
ITS 1%
ITS 1% + TGF-ß1 (10ng/ml)
D28
D56
Cellular viability (%)
100
95
90
85
10
0
Col0
Col0.5
Col1
Col5
Col0
Col0.5
Col1
Col5

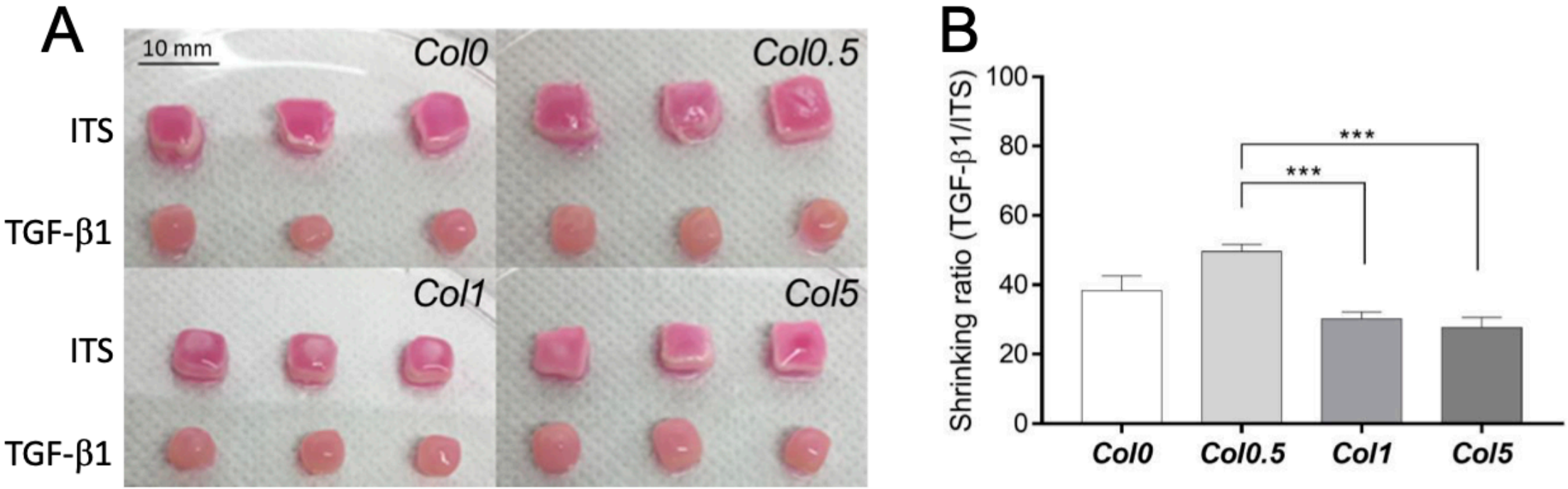
A
10 mm
Col0
Col0.5
Col1
Col5
ITS
TGF-β1
ITS
TGF-β1
B
Shrinking ratio (TGF-β1/ITS)
100
80
60
40
20
0
***
***
Col0
Col0.5
Col1
Col5

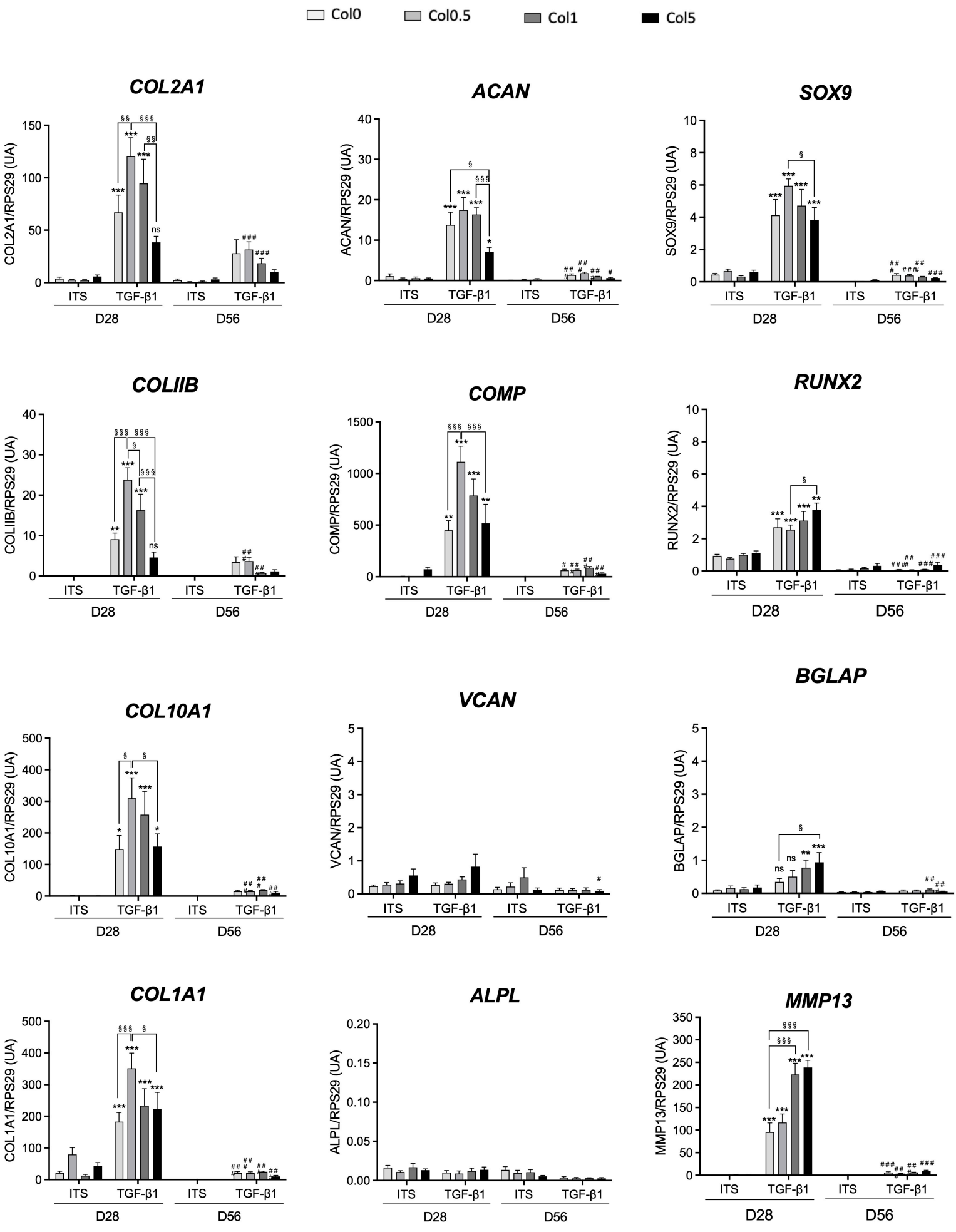
Col0
Col0.5
Col1
Col5
COL2A1
COL2A1/RPS29 (UA)
ACAN
ACAN/RPS29 (UA)
SOX9
SOX9/RPS29 (UA)
COLIIB
COLIIB/RPS29 (UA)
COMP
COMP/RPS29 (UA)
RUNX2
RUNX2/RPS29 (UA)
COL10A1
COL10A1/RPS29 (UA)
VCAN
VCAN/RPS29 (UA)
BGLAP
BGLAP/RPS29 (UA)
COL1A1
COL1A1/RPS29 (UA)
ALPL
ALPL/RPS29 (UA)
MMP13
MMP13/RPS29 (UA)
ITS
TGF-β1
D28
D56

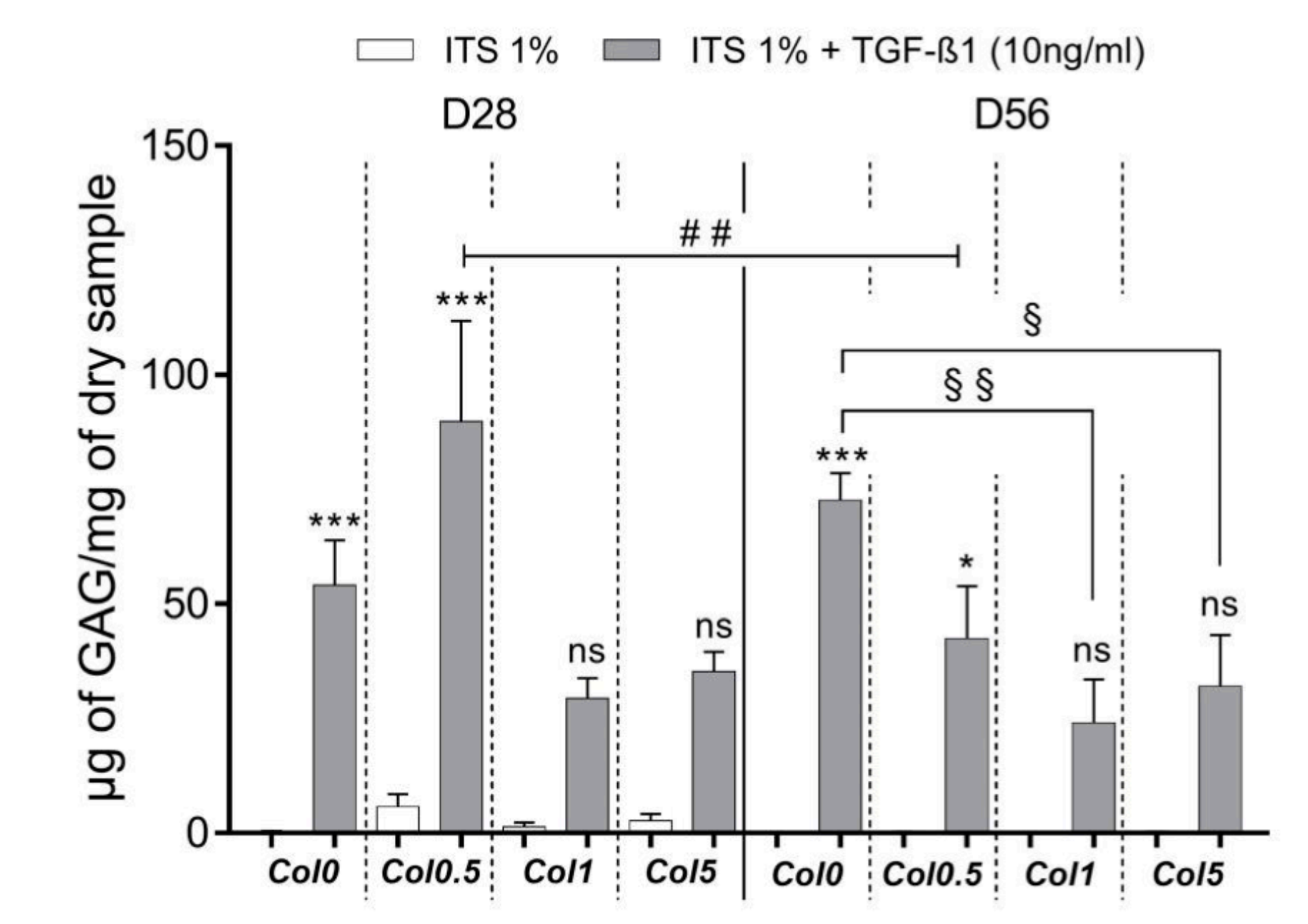
ITS 1%
ITS 1% + TGF-ß1 (10ng/ml)
D28
D56
µg of GAG/mg of dry sample
150
100
50
0
# #
§
§ §
***
***
***
*
ns
ns
ns
ns
Col0
Col0.5
Col1
Col5
Col0
Col0.5
Col1
Col5

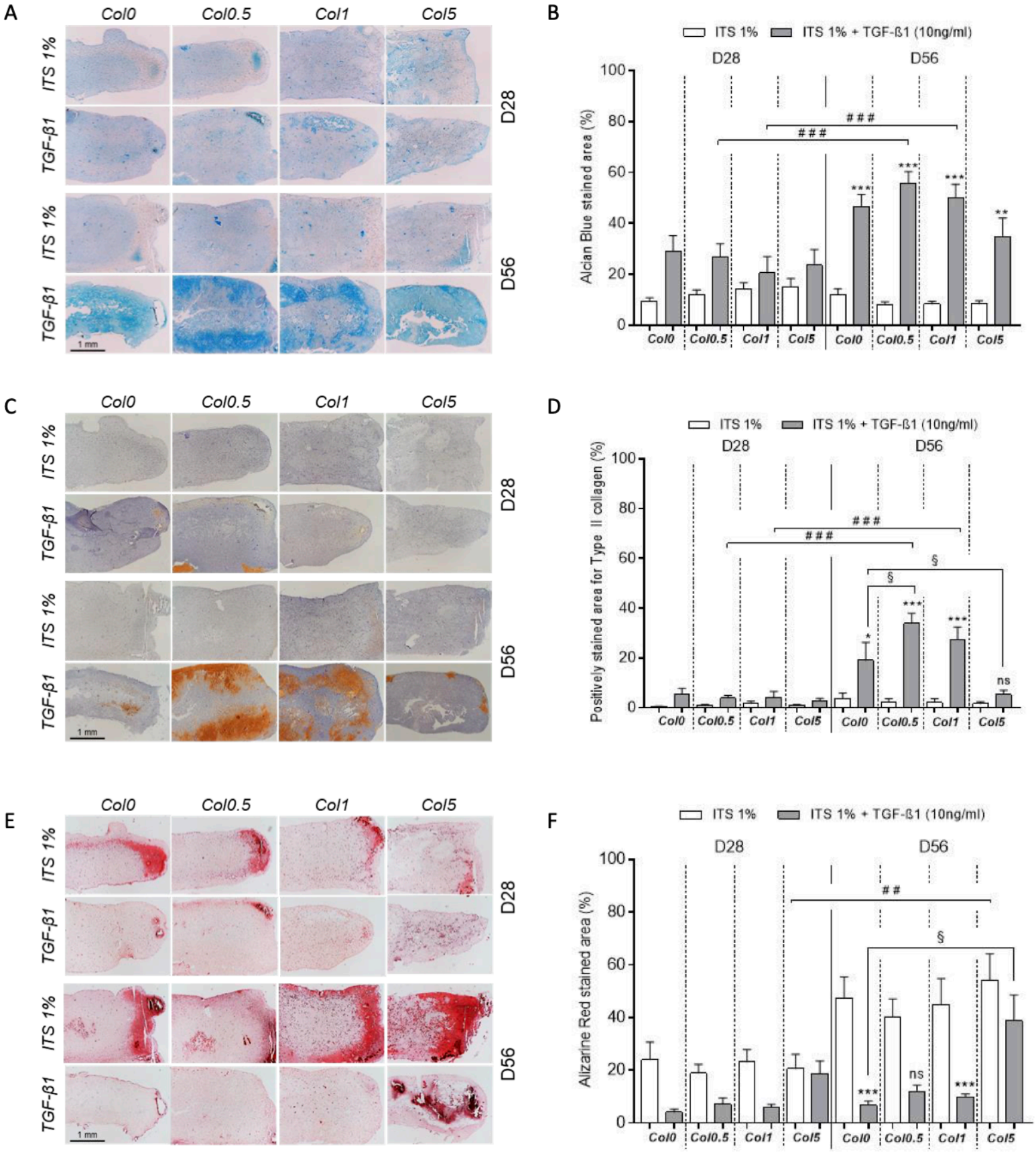
A
Col0
Col0.5
Col1
Col5
ITS 1%
TGF-ß1
D28
D56
1 mm
B
ITS 1%
ITS 1% + TGF-ß1 (10ng/ml)
D28
D56
Alcian Blue stained area (%)
100
80
60
40
20
0
###
***
**
Col0
Col0.5
Col1
Col5
C
D
Positively stained area for Type II collagen (%)
§
*
ns
E
F
Alizarine Red stained area (%)
##

Supplementary data 1: Previous studies using type I Collagen in hydrogels for cartilage engineering

Reference	Collagen quantity added	Other bioinks component	Cellular		Type of experiment
			Cell type	Species	
Beketov et al, 2021 [1]	0.04 mg/mL	Collagen buffer solution	Chondrocyte	Rat	*in vivo*
Lee et al, 2018 [2]	0.05 mg/mL	/	Preosteoblasts	Mouse	*in vitro*
Sanz-Ramos et al, 2014 [3]	1 ; 2 or 3 mg/mL	/	Chondrocytes	Rat	*in vitro*
			Chondrocytes	Sheep	*in vivo*
Yang et al, 2018 [4]	3 mg/mL	Alginate	Chondrocytes	Rat	*in vitro*
Yang et al, 2018 [5]	6 mg/mL	Methacrylated Hyaluronic acid Methacrylated icariin	Bone marrow mesenchymal stem cells	Rabbit	*in vitro*
Zheng et al, 2009 [6]	7 mg/mL	/	Chondrocytes	Rabbit	*in vivo*
Yuan et al, 2014 [7]	7 mg/mL	/	Chondrocytes	Rabbit	*in vitro*
Lee et al, 2021 [8]	40 mg/mL	Proanthocyanidin Oxidized hyaluronic acid	/	/	*in vivo*

References :

[1] Beketov, E.E.; Isaeva, E.V.; Yakovleva, N.D.; Demyashkin, G.A.; Arguchinskaya, N.V.; Kisel, A.A.; Lagoda, T.S.; Malakhov, E.P.; Kharlov, V.I.; Osidak, E.O.; et al. Bioprinting of Cartilage with Bioink Based on High-Concentration Collagen and Chondrocytes. *Int J Mol Sci* **2021**, *22*, 11351, doi:10.3390/ijms222111351.1.

[2] Lee, J.; Yeo, M.; Kim, W.; Koo, Y.; Kim, G.H. Development of a Tannic Acid Cross-Linking Process for Obtaining 3D Porous Cell-Laden Collagen Structure. *Int J Biol Macromol* **2018**, *110*, 497–503, doi:10.1016/j.ijbiomac.2017.10.105.

[3] Sanz-Ramos, P.; Duart, J.; Rodríguez-Goñi, M.V.; Vicente-Pascual, M.; Dotor, J.; Mora, G.; Izal-Azcárate, I. Improved Chondrogenic Capacity of Collagen Hydrogel-Expanded Chondrocytes: In Vitro and in Vivo Analyses. *J Bone Joint Surg Am* **2014**, *96*, 1109–1117, doi:10.2106/JBJS.M.00271.

[4] Yang, X.; Lu, Z.; Wu, H.; Li, W.; Zheng, L.; Zhao, J. Collagen-Alginate as Bioink for Three-Dimensional (3D) Cell Printing Based Cartilage Tissue Engineering. *Mater Sci Eng C Mater Biol Appl* **2018**, *83*, 195–201, doi:10.1016/j.msec.2017.09.002.

[5] Yang, J.; Liu, Y.; He, L.; Wang, Q.; Wang, L.; Yuan, T.; Xiao, Y.; Fan, Y.; Zhang, X. Icariin Conjugated Hyaluronic Acid/Collagen Hydrogel for Osteochondral Interface Restoration. *Acta Biomater* **2018**, *74*, 156–167, doi:10.1016/j.actbio.2018.05.005.

[6] Zheng, L.; Sun, J.; Chen, X.; Wang, G.; Jiang, B.; Fan, H.; Zhang, X. In Vivo Cartilage Engineering with Collagen Hydrogel and Allogenous Chondrocytes after Diffusion Chamber Implantation in Immunocompetent Host. *Tissue Eng Part A* **2009**, *15*, 2145–2153, doi:10.1089/ten.tea.2008.0268.

[7] Yuan, T.; Zhang, L.; Li, K.; Fan, H.; Fan, Y.; Liang, J.; Zhang, X. Collagen Hydrogel as an Immunomodulatory Scaffold in Cartilage Tissue Engineering. *J Biomed Mater Res B Appl Biomater* **2014**, *102*, 337–344, doi:10.1002/jbm.b.33011.

[8] Lee, C.-F.; Hsu, Y.-H.; Lin, Y.-C.; Nguyen, T.-T.; Chen, H.-W.; Nabilla, S.C.; Hou, S.-Y.; Chang, F.-C.; Chung, R.-J. 3D Printing of Collagen/Oligomeric Proanthocyanidin/Oxidized Hyaluronic Acid Composite Scaffolds for Articular Cartilage Repair. *Polymers (Basel)* **2021**, *13*, 3123, doi:10.3390/polym13183123.

Supplementary Data #2: Rheological properties of the studied bioinks

Methods. Experimental results were obtained by the use of stress-controlled rheometer (Discovery HR2, TA Instruments, USA) with a flow sweep procedure from 100s^{-1} to 0.1 s^{-1} and a 40mm parallel plates geometries. The gap between the top and bottom geometries was defined at 850 µm. To avoid drying effect of hydrogels during rheological testing, the top geometry was equipped with a water trap and enclose by a plate cover.

The rheological behavior of collagen-based hydrogels were described as yield stress fluid according to Hesrshel-Bulkley (H-B) model (Equation 1). Numerical fitting was performed on TRIOS software (v5.1, TA instruments, USA) to define parameters for each hydrogels (Table 1).

Equation 1 : $\tau = \tau_0 + k\dot{\gamma}^n$. Where τ is the shear stress in Pa, τ_0 the yield stress in Pa, k the consistency index in Pa^n and n the flow index (-)

Results. As demonstrated in previous works (1-3), the variation of the H-B parameters are too small (*e.g.* $\tau_0 \in [20\,;\,50]$Pa), to be considered as impacting in EBB.

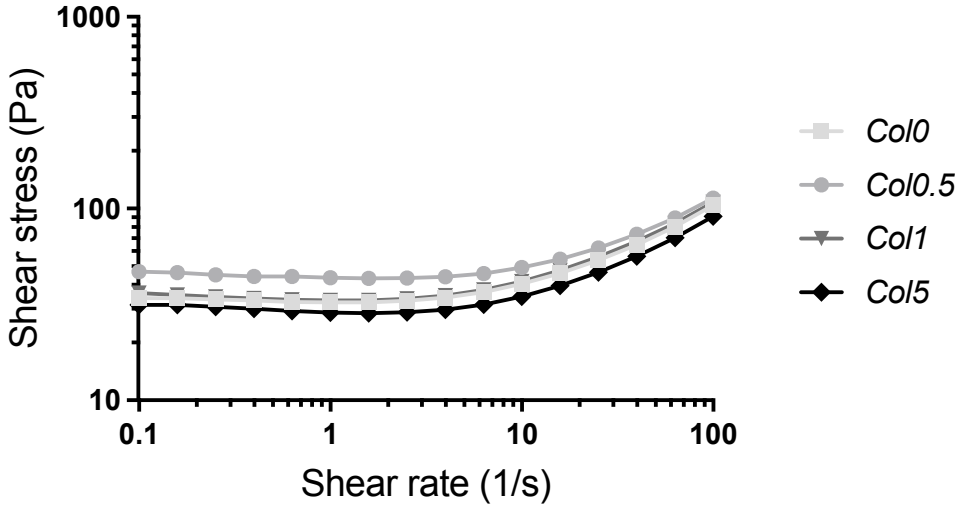

Figure 1 : Rheological behavior (Shear stress vs Shear rate) of collagen-based hydrogels (standard deviation less than 3%).

Table 1 : H-B parameters describing the rheological properties of collagen-based hydrogels.

H-B parameters	Col0	Col0.5	Col1	Col5
τ_0 (Pa)	32.06	43.59	33.02	21.56
k (Pa^n)	1.120	0.690	1.192	1.580
n (-)	0.906	1.006	0.901	0.817

1. Courtial, E.-J., Perrinet, C., Colly, A., Mariot, D., Frances, J.-M., Fulchiron, R., Marquette, C., (2019). Silicone rheological behavior modification for 3D printing: Evaluation of yield stress impact on printed object properties. Additive Manufacturing. 28:50-57 http://doi.org/https://doi.org/10.1016/j.addma.2019.04.006.
2. Lopez, A., Marquette, C.A., Courtial, EJ. FingerMap: a new approach to predict soft material 3D objects printability. *Prog Addit Manuf* **6**, 53–62 (2021). https://doi.org/10.1007/s40964-020-00143-5
3. Lemarié, L., Anandan, A., Petiot, E., Marquette, C., Courtial, E.-J., (2021). Rheology, simulation and data analysis toward bioprinting cell viability awareness. Bioprinting. 21:e00119. http://doi.org/https://doi.org/10.1016/j.bprint.2020.e00119.

Supplementary data 3: Macroscopical aspects of EBB constructs

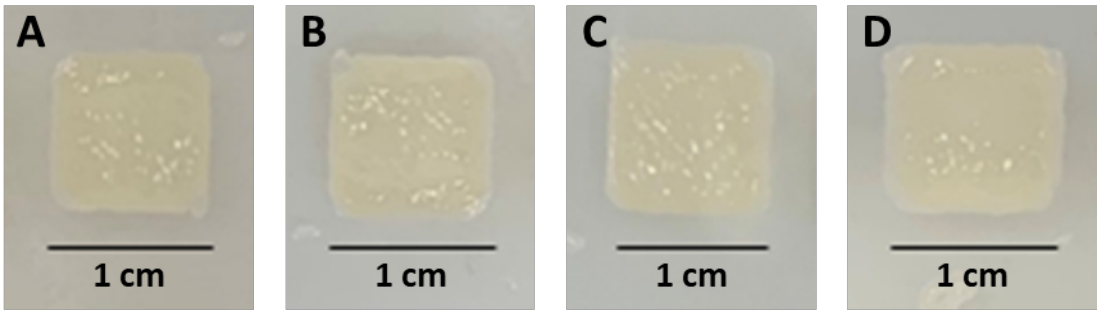

Constructs with a final size of 1 cm × 1 cm and four consecutive layers were extruded at 28°C using a 3D bioprinter. We inspected each construct printed visually. Photographs of the constructs post-printing, before their polymerization, were taken for the Col0 (A), Col0.5 (B), Col1 (C), and Col5 (D) bioinks. All printed substitutes showed defined and reproducible structures, similar to the initial design regardless of the bioink composition without geometric imperfection (rectangular shapes with a length of 1 cm, a width of 1 cm, and a thickness of 4 mm, corresponding to the deposition of 4 consecutive layers). These observations agree with the rheology studies, which do not show any significant difference between the four bioinks.

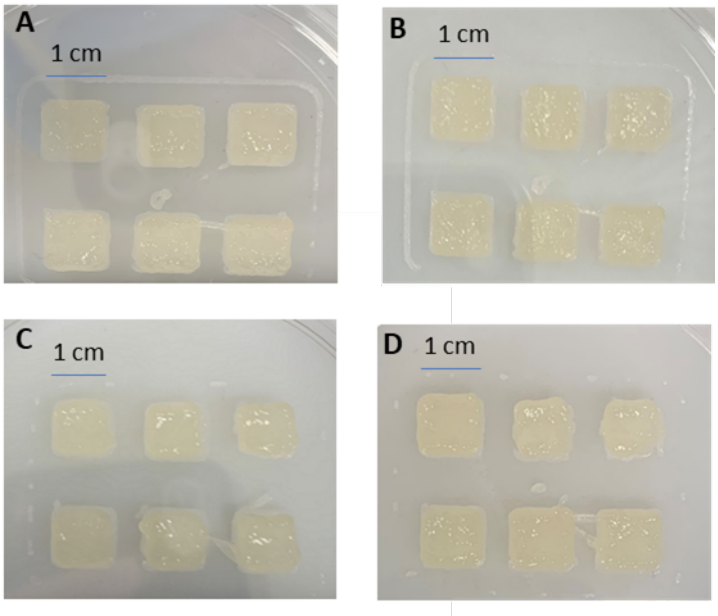

Macroscopical repeatability of the process

Supplementary Data 4: Quantitative real-time PCR primers

Gene		Primer sequences	Annealing temperature (°C)	Amplicon size (bp)	Accession number
RPS29	Fwd	5′-AGATGGGTCACCAGCAGCTGTACTG-3′	60	73	NM_001032
	Rev	5′- AGACACGACAAGAGCGAGAA -3′			
COL2A1	Fwd	5′-ATGACAATCTGGCTCCCAAC-3′	55	200	NM_001844
	Rev	5′-GAACCTGCTATTGCCCTCTG-3′			
COLIIB	Fwd	5′-GCATGAGGGCGCGGTAGAGA-3′	70	195	NM_033150.2
	Rev	5′-TGGTCCTGGTTGCCGGACAT-3′			
SOX9	Fwd	5′-GAGCAGACGCACATCTC-3′	55	118	NM_000346
	Rev	5′-CCTGGGATTGCCCCGA-3′			
ACAN (Aggrecan)	Fwd	5′-TCGAGGACAGCGAGGCC-3′	63	85	NM_001135
	Rev	5′-TCGAGGGTGTAGCGTGTAGAGA-3′			
COMP	Fwd	5′-ACAATGACGGAGTCCCTGAC-3′	60	115	NM_000095
	Rev	5′-TCTGCATCAAAGTCGTCCTG-3′			
VCAN (Versican)	Fwd	5′-TGTTCCTCCCACTACCCTTG-3′	62	122	NM_001164098
	Rev	5′-CTTCCACAGTGGGTGGTCTT-3′			
COL1A1	Fwd	5′- AGGTGCTGATGGCTCTCCT-3′	60	104	NM_000088
	Rev	5′- GGACCACTTTCACCCTTGT -3′			
COL10A1	Fwd	5′-GCTAAGGGTGAAAGGGGTTC-3′	60	118	NM_000493
	Rev	5′-CTCCAGGATCACCTTTTGGA-3′			
RUNX2	Fwd	5′-CCCGTGGCCTTCAAGGT-3′	60	73	NM_001278478
	Rev	5′-CGTTACCCGCCATGACAGTA-3′			
ALPL (Alkaline Phosphatase)	Fwd	5′-GGTGAACCGCAACTGGTACT-3′	62	187	NM_001632
	Rev	3′-CCCACCTTGGCTGTAGTCAT-3′			
MMP13	Fwd	5′-TGGTGGTGATGAAGATGATTT-3′	60	162	NM_002427
	Rev	5′TCTAAGCCGAAGAAAGACTGC-3′			
BGLAP (osteocalcin)	Fwd	5′-GTGCAGAGTCCAGCAAAGGT-3′	62	175	NM_199173
	Rev	5′-TCAGCCAACTCGTCACAGTC-3′			